

pubs.acs.org/JPCA Article

# Two-Color IRMPD Applied to Conformationally Complex Ions: Probing Cold Ion Structure and Hot Ion Unfolding

Published as part of The Journal of Physical Chemistry virtual special issue "Dor Ben-Amotz Festschrift".

Christopher P. Harrilal, Andrew F. DeBlase, Scott A. McLuckey,\* and Timothy S. Zwier\*



Cite This: J. Phys. Chem. A 2021, 125, 9394-9404



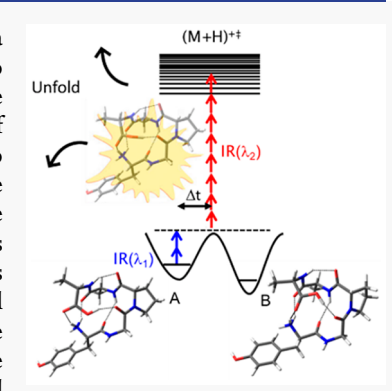
ACCESS

Metrics & More



s Supporting Information

ABSTRACT: Two-color infrared multiphoton dissociation (2C-IRMPD) spectroscopy is a technique that mitigates spectral distortions due to nonlinear absorption that is inherent to one-color IRMPD. We use a 2C-IRMPD scheme that incorporates two independently tunable IR sources, providing considerable control over the internal energy content and type of spectrum obtained by varying the trap temperature, the time delays and fluences of the two infrared lasers, and whether the first or second laser wavelength is scanned. In this work, we describe the application of this variant of 2C-IRMPD to conformationally complex peptide ions. The 2C-IRMPD technique is used to record near-linear action spectra of both cations and anions with temperatures ranging from 10 to 300 K. We also determine the conditions under which it is possible to record IR spectra of single conformers in a conformational mixture. Furthermore, we demonstrate the capability of the technique to explore conformational unfolding by recording IR spectra with widely varying internal energy in the ion. The protonated peptide ions YGGFL (NH<sub>3</sub><sup>+</sup>-Tyr-Gly-Phe-Leu, Leu-enkephalin) and YGPAA (NH<sub>3</sub><sup>+</sup>-Tyr-Gly-Pro-Ala-Ala) are used as model systems for exploring the advantages and disadvantages of the method when applied to conformationally complex ions.



## I. INTRODUCTION

Mass spectrometry coupled to laser spectroscopy is a powerful tool for structure elucidation of ions. Often, the gas-phase ions of interest are held together by networks of intramolecular H-bonds. In the case of peptide ions, these networks involve both amide—amide H-bonds and the electrostatically driven H-bonding interactions between the charge site(s) and various acceptor groups. As soon as these ions are more than a few residues in length, the competition between various possible arrangements of the H-bonds and the small energy differences associated with a room temperature Boltzmann distribution make it difficult or impossible to chemically intuit which structures will be formed.

The field of gas-phase ion spectroscopy continues to grow in its reach and insight into ion structure. The ready-made ability to mass-select reactants and selectively detect fragment ion products makes action spectroscopy built around ion fragmentation the method of choice for such studies. <sup>1-6</sup> Infrared multiple photon dissociation (IRMPD), <sup>7-11</sup> messenger tagging, <sup>12-15</sup> and IR-UV double resonance <sup>1,16-18</sup> (IR-UV DR) are commonly used action-based techniques for probing the H-bonded networks present in gas phase ions. Each technique produces an IR spectrum that provides insights about the functionalities, intramolecular, and intermolecular interactions. <sup>10</sup> When peptide ions are the subject of study, the IR spectrum probes the hydrogen-bonded network that is present. Hydrogen-bond donor (e.g., N–H) and acceptor

(e.g., C=O) groups have the frequencies of their vibrational fundamentals shifted by the strength and orientation of the H-bond(s) in which they are involved and the couplings between them. Thus, the resulting experimental spectrum reflects in a sensitive manner the three-dimensional structure of the ion and when combined with theory allows for explicit structural assignments to be made. 1,19

Because these techniques are action-based and indirectly probe the infrared absorptions of the ions, it is important that the experimental conditions used do not skew the resulting IR spectra. <sup>8,9</sup> Generally, suitable conditions can be achieved by limiting the fluence of the tuned IR laser. <sup>20</sup> In messenger tagging and IR-UV DR, ions are often cryo-cooled prior to being probed, making it possible to preserve the innate spectral characteristics of the single-photon absorption spectrum by probing fragmentation after absorption of one or a small number of IR photons. <sup>1,21,22</sup> At higher powers where multiphoton processes play a major role, the resulting spectra can be distorted in intensity and can even result in certain

Received: September 24, 2021 Published: October 13, 2021





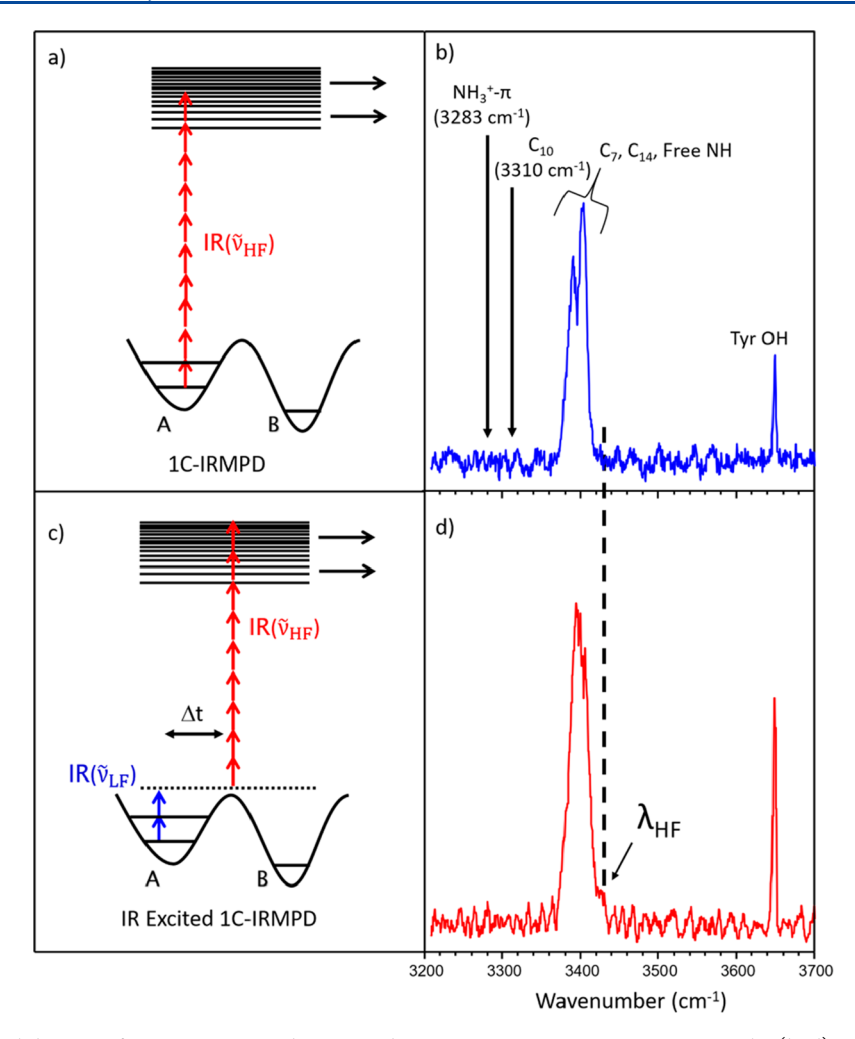


Figure 1. (a, c) Energy level diagrams for 1C-IRMPD and IR excited 1C-IRMPD spectroscopies, respectively. (b, d) IR spectra of [YGGFL + H]<sup>+</sup> over the 3200–3700 cm<sup>-1</sup> region resulting from 1C-IRMPD on the nonexcited and IR-excited ion, respectively. The wavenumber positions of two absent IR transitions are shown in (b). The spectrum in (d) was recorded with the low-fluence laser (blue in c) fixed at 3400 cm<sup>-1</sup> with a 30 ns delay between the two IR sources; that is,  $[\lambda_{LF}(3400 \text{ cm}^{-1})|30 \text{ ns}|\lambda_{HF}(\text{tuned})]$ . See the text for further discussion.

vibrational bands vanishing from the spectrum. <sup>23,24</sup> In typical IRMPD spectra, this is often of more concern as the mechanism for inducing fragmentation relies on the absorption of multiple infrared photons at each vibrational mode. Previous analysis has shown this process to have a minimal effect on the resulting spectra of rigid ions, allowing for accurate modeling of the observed spectral deviations. <sup>9,25</sup> In more flexible peptide ions, however, there can be a noticeable difference between spectra recorded by using IRMPD compared to IR-UV DR and messenger tagging. <sup>26</sup> These deviations can be harder to interpret or predict and make it more difficult to accurately make structural assignments based on harmonic level calculations.

Previous comparisons between infrared photodissociation (IRPD) and IRMPD on clusters correlate missing bands in the IRMPD spectra (called 'IRMPD transparency') to shifts in resonant frequencies during the early stages of IRMPD. <sup>23,24</sup> The shifts in frequency are proposed to result from a disruption in the hydrogen-bonded network at energies below dissociation. The degree of IRMPD transparency is reduced as the dissociation limit approaches the amount of energy imparted by a single IR photon. <sup>23</sup>

In flexible systems, if some fraction of the IR bands in the spectrum are transparent in IRMPD, it would be difficult or

impossible to assign the resulting IRMPD spectrum to a particular conformation. Peptides represent a class of molecules that are conformationally complex and require absorption of many IR photons before fragmentation is kinetically competitive relative to isomerization. This combination is especially susceptible to IR transparency.

An alternative but less common technique to record gas phase IR spectra is two-color IRMPD (2C-IRMPD). 27-29 This pump-probe technique divides the IRMPD process into two irradiation steps. The first laser, which is tunable, is set to a lower fluence and used to vibrationally excite ions while the second laser, set to high fluence conditions, induces dissociation selectively from the subset of ions that have absorbed one or more IR photons.30,31 This method was initially developed by Lee and co-workers in their studies of protonated water clusters.<sup>27</sup> In the early version of this technique a line-tunable CO2 laser was used to enhance the dissociation yield after irradiation with a tunable IR light source. More recently, the groups of Niedner-Schatteburg<sup>32</sup> and Johnson<sup>34–36</sup> have employed a variant of this technique which makes use of two tunable optical parametric oscillator/ amplifier (OPO/OPA) IR lasers to record the vibrational spectra of metalated ions and protonated water clusters. In this variation both lasers can be tuned, providing additional

versatility. The advantage of this technique over single-color IRMPD is that it can detect vibrational bands that are prone to IRMPD transparency. However, in these studies either the dissociation energy or conformational flexibility was limited.

In the present work, we demonstrate the ability to apply a similar 2C-IRMPD scheme to conformationally complex protonated peptide ions, circumventing issues associated with IRMPD transparency. The technique is initially tested on wellcharacterized protonated pentapeptides to gauge its feasibility when applied to ions of this size regime (~500 Da). We report conditions under which 2C-IRMPD is possible on these prototypical peptide ions and explore the circumstances under which undistorted, near-linear spectra of cold/room temperature ions can be recorded. In addition to successfully obtaining near-linear spectra, we demonstrate the use of alternative 2C-IRMPD schemes to gain new insights into the peptide conformational isomerization that precedes fragmentation. In particular, we examine the effects of internal energy on the 2C-IRMPD spectra, ranging from thermal energies to energies well above the fragmentation threshold. These latter spectra represent snapshots of the peptide ion "unfolding" during the delay between the two IR pulses. A comparison of the 2C-IRMPD spectra recorded under the whole range of internal energies reveals which vibrational bands are most sensitive to the ion's internal energy content. This, in turn, establishes an experimentally verified link in peptide ions between conformational isomerization and IRMPD transparency. Lastly, we show results for a first attempt to obtain conformation-specific IR spectra by using 2C-IRMPD, an ability of considerable value to spectroscopic studies of gas phase ions. As we will see, the conditions under which conformation-specific 2C-IRMPD spectra can be obtained are established but are restrictive enough that it may not always be possible to meet the needed criteria.

## II. EXPERIMENTAL METHODS

All spectra were recorded on a custom-built apparatus that is composed of a tandem triple quadrupole mass spectrometer on one axis with an orthogonal spectroscopy axis mounted between the second and third quadrupoles.<sup>37</sup> Methods for recording UV and IR-UV DR spectra are described elsewhere.<sup>2</sup> Briefly, ions are generated via nano-electrospray ionization (n-ESI) and guided into a linear quadrupole ion trap. The ion of interest is mass isolated by using RF-DC isolation and then guided via a turning quadrupole down the spectroscopy axis where the ions are trapped in a cryogenically cooled octupole ion trap. The trap is held at 5 K via a close cycle helium cryostat (Sumitomo Heavy Industries). Ions are cooled to ~10 K via collisions with the He buffer gas before spectroscopic interrogation by two counterpropagating lasers. The laserinduced photofragments are extracted back down the spectroscopy axis and turned into a final linear ion trap. The residual precursor ions are ejected from the trap via a supplemental auxiliary waveform calculated with the SX wave software,<sup>38</sup> and the remaining photofragments are extracted onto a channeltron detector.

The 2C-IRMPD scheme is applied in an analogous manner to that of IR-UV double resonance, which has been previously described. To acquire a near-linear 2C-IRMPD spectra, the 1C-IRMPD spectrum of the nonexcited and IR-excited ion must first be known. The schemes to obtain these spectra are graphically illustrated in Figures 1a and 1c, respectively. In this approach the 1C-IRMPD spectrum

(Figure 1b) is obtained by irradiating the ion packet with a single pulse of a high-fluence tuned IR laser. The conditions for the high-fluence laser, termed  $\lambda_{HE}$ , are 30 mJ/pulse, focused to the center of the trap with a 50 cm focal lens. In this mode, it is required to induce photofragmentation with a single laser pulse. In order for our nanosecond IR laser to induce photofragmentation at a particular wavelength, the laser fluence must be sufficient to cause absorption of multiple IR photons of the same wavelength, thereby reaching ion internal energies at which fragmentation occurs prior to collisional stabilization of the IR excited ion in the cold trap. Cooling times have been previously measured to occur on the milliseconds time scale. 40 Efficient "ladder climbing" occurs when the peak wavelength of a particular IR absorption does not change significantly with internal energy in the ion, so that successive  $v'' \rightarrow v'' + 1$  transitions can occur, leading, in turn, to efficient fragmentation.<sup>23</sup> Bands that shift their frequency out of resonance with increasing internal energy will become "IR transparent" and will be observed with greatly reduced intensity or disappear completely from the 1C-IRMPD spectrum.

To record the 1C-IRMPD spectrum of the IR-excited ions (Figure 1d), a low-fluence laser termed  $\lambda_{LF}$  (~15 mJ/pulse resized to 6 mm diameter as it passes through the ion packet) is fixed on a transition identified in the 1C-IRMPD spectrum, while the  $\lambda_{\rm HF}$  is scanned across the spectral region. As the fluence of this laser is significantly lower than the high-fluence laser, it is possible to vibrationally heat the ion without inducing fragmentation. The temporal delay between the two lasers is typically set to 30 ns, with  $\lambda_{LF}$  preceding  $\lambda_{HF}$ . The spectrum of the IR excited ion (Figure 1d) serves to identify absorptions that are unique to the IR-excited ion relative to the nonexcited ion. In what follows, we use a shorthand notation for the 2C IRMPD laser schemes  $[\lambda_1(\text{tuned/fixed})|X]$  nsl  $\lambda_2$ (tuned/fixed)] and designate which laser is fixed versus tuned and the time delay between them. The laser that irradiates the ion packet first is always listed first.

To record near-linear 2C-IRMPD spectra, the same scheme shown in Figure 1c is used; however,  $\lambda_{\rm HF}$  is fixed and  $\lambda_{\rm LF}$  is scanned.  $\lambda_{\rm HF}$  is fixed on a unique transition present in the spectrum of the IR excited ion, such that no fragmentation occurs, unless the ion first absorbs a photon from the low fluence laser. Careful control of the fluence of this laser results in near-linear IR spectra. As both lasers are tunable, different types of spectra can be generated depending on the relative timings between lasers as well as which is tuned and which is fixed. These spectra will be explained in turn in the following section.

## III. RESULTS AND DISCUSSION

**10 K** [YGGFL + H]<sup>+</sup>. 1C-IRMPD on Nonexcited and IR-Excited lons. Many of the initial experiments using 2C-IRMPD were performed on protonated YGGFL, which our group has studied in some detail previously by using the complementary method of IR-UV double-resonance spectroscopy (IR-UV DR). The IR spectrum of the cryo-cooled ion with  $T_{\rm vib} \sim 10$  K will be used to compare against the 2C-IRMPD results. Based on a comparison of the experimental and calculated IR spectra, [YGGFL + H]<sup>+</sup> was shown to funnel all its population into the single H-bonded conformation shown in Figure 2, a charge-stabilized type II' β-turn.

Initially, the 1C-IRMPD spectrum of [YGGFL + H]<sup>+</sup> was recorded at 10 K (Figure 1b). This 1C-IRMPD spectrum

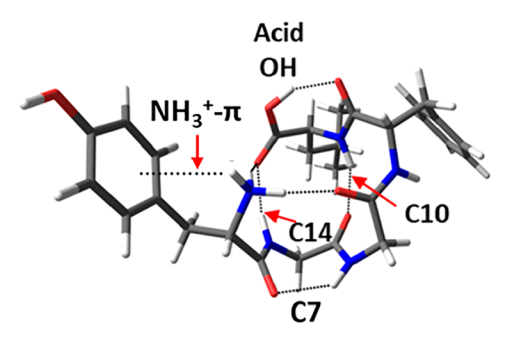


Figure 2. Previously assigned structure of protonated YGGFL with labeled hydrogen bonds. Adapted from refs 2 and 41.

shows three bands over the  $3200-3700~{\rm cm}^{-1}$  region, including a closely spaced doublet near  $3400~{\rm cm}^{-1}$  and a single sharp transition at  $3650~{\rm cm}^{-1}$ . These bands are assigned to the C7 and C14 NH stretch fundamentals and the free Tyr OH stretch fundamental, based on the close correspondence between experiment and the calculated spectrum for the conformer shown in Figure 2. By comparison, Figure 3b shows the near-linear spectrum of the [YGGFL + H]<sup>+</sup> ion recorded by using IR-UV DR at 10 K. Note from Figure 1b that the NH stretch fundamentals due to the NH group in a 10-membered H-bonded ring (C10) and the  $\pi$ -bound NH<sub>3</sub><sup>+</sup> NH stretch are completely missing from the 1C-IRMPD spectrum under the laser power conditions used to record the spectrum. Aside from insufficient laser power, missing bands are ultimately the

result of absorption of too few IR photons due to IRMPD transparency.

Using the 2C-IRMPD scheme illustrated in Figure 1c,  $[\lambda_{\rm LF}(3400~{\rm cm}^{-1})|30~{\rm ns}|\lambda_{\rm HF}({\rm tuned})]$ , it is possible to record the spectrum of the IR-excited ions (Figure 1d). As discussed below, it is estimated that  $\lambda_{\mathrm{LF}}$  delivers one to two photons to the ion when on resonance. The spectrum recorded in this manner provides a sensitive measure of the spectral differences between the 10K 1C spectrum and the 1C spectrum of an ion with at least 3400 cm<sup>-1</sup> of internal energy. To put the differences in energy content into perspective, while the large majority of the YGGFL ions at 10 K are in the vibrational zeropoint level ( $E_{\rm ave} \sim 3~{\rm cm}^{-1}$ ), the average internal energy at 300 K is calculated to be 6700 cm<sup>-1</sup>. Comparison of the two spectra in Figures 1b and 1d reveals them to be highly similar. Besides a loss of resolution in the closely spaced doublet, the black dashed line highlights a more subtle broadening that produces a small shoulder at 3420 cm<sup>-1</sup>. An overlay of these two spectra is given in Figure S1a. This slight spectral broadening after the absorption of a limited number of photons is crucial for the 2C-IRMPD technique to be feasible when applied to molecular ions in this size regime, since it provides the wavelength to fix  $\lambda_{HF}$  that is absorbed only by ions that have been vibrationally excited by  $\lambda_{LF}$ .

Note that even with the additional starting internal energy imparted with  $\lambda_{\text{LF}}$ , the NH<sub>3</sub><sup>+</sup>- $\pi$  and C10 NH stretch transitions are still absent from the spectrum. The 1C spectrum recorded at 300 K (Figure S1b) shows the presence of a weak NH<sub>3</sub><sup>+</sup>- $\pi$ 

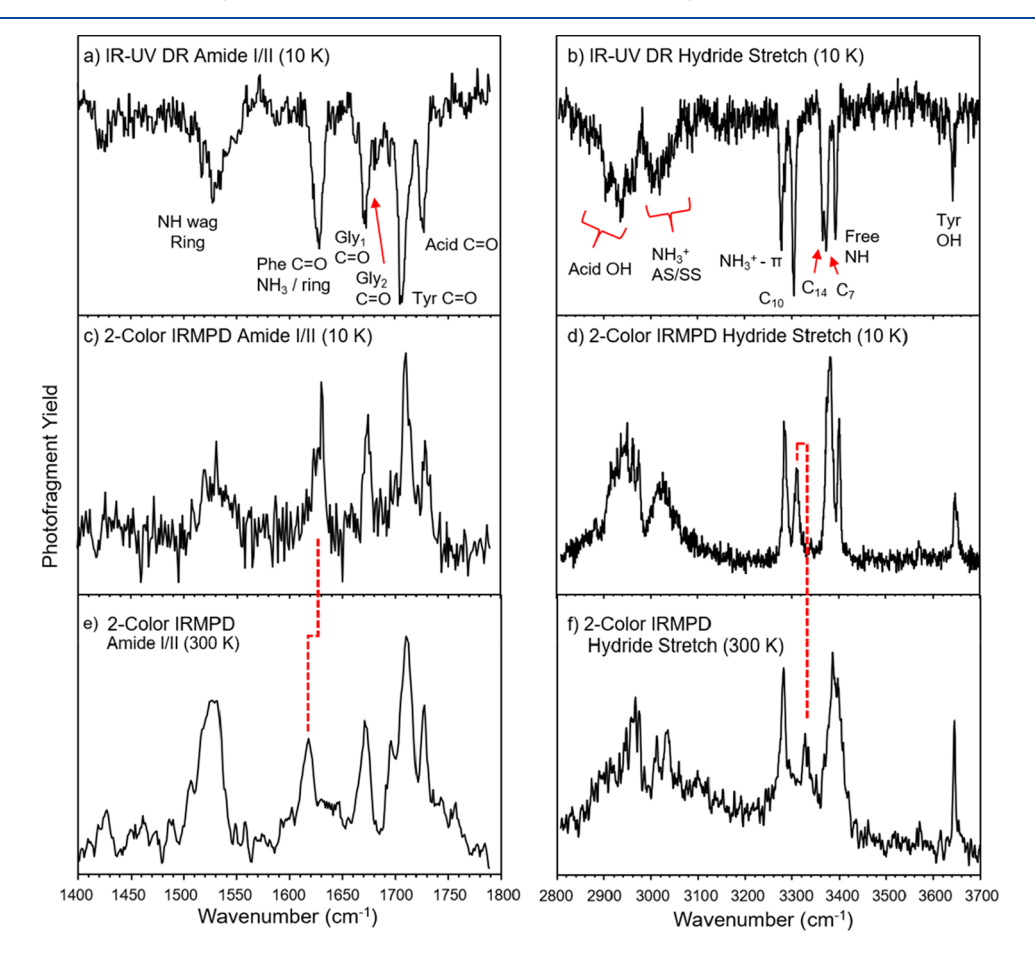


Figure 3. Near-linear IR-UV DR spectra of  $[YGGFL + H]^+$  recorded at 10 K in the amide I/II (a) and hydride stretch region (b). Near-linear 2C-IRMPD spectra recorded in the amide I/II and hydride stretch regions at 10 K (c, d) and at 300 K (e, f).

band, suggesting that the absence of this band when starting at  $10~\rm K$  is due to our choice of laser power for  $\lambda_{\rm LF}$ . The absence of the  $\rm NH_3^+$ - $\pi$  band in the spectrum of the IR-excited ions (Figure 1d) can be used to gauge how many photons are absorbed when  $\lambda_{\rm LF}$  is fixed at  $3400~\rm cm^{-1}$ . While the Boltzmann distribution at  $300~\rm K$  is clearly different than the delta function in energy produced by absorption of an IR photon, we surmise from the absence of the  $\rm NH_3^+$ - $\pi$  transition that the focusing conditions for  $\lambda_{\rm LF}$  used in these experiments deliver an internal energy increase to the ion of less than two IR photons (the average internal energy at  $300~\rm K$ ). We will return to the absence of the C10 band when discussing the spectral effects of IRMPD transparency.

2C-IRMPD Spectra at 10 K. The 2C-IRMPD scheme used to record the spectrum of the IR-excited ions displayed in Figure 1d can be modified from  $[\lambda_{LF}(3400 \text{ cm}^{-1})]+30$  $nsl\lambda_{HF}(tuned)$ ] to  $[\lambda_{LF}(tuned)$ l+30  $nsl\lambda_{HF}(3420~cm^{-1})]$  to record the near-linear 2C spectra displayed in Figures 3c and 3d. By setting  $\lambda_{\rm HF}$  at 3420 cm<sup>-1</sup>, absorption occurs only in ions that have been excited with  $\lambda_{\rm LF}$ . This scheme thereby limits the amount of spectral distortion, as all vibrational bands can be measured without the need to induce dissociation through excitation of each mode. The near-linear spectra shown in Figures 3c and 3d are taken at an initial ion temperature of 10 K, scanning in the amide I/II and hydride stretch regions, respectively. The scans directly above Figures 3a and 3b are the near-linear IR-UV DR spectra taken at 10 K in the same regions. Note that the 2C-IRMPD spectra are very similar the IR-UV DR spectra, convincingly demonstrating the applicability of the 2C-IRMPD scheme to circumvent issues of IRMPD transparency and faithfully reporting the IR spectrum of conformationally complex ions in the 500 Da regime at 10

While the spectra in Figures 3d and 3b are very similar, close inspection does reveal small but reproducible differences. In particular, the intensity of the C10 NH stretch band is reduced in the 2C spectrum, when comparing it to the surrounding NH<sub>3</sub><sup>+</sup>- $\pi$ , C14, C7, and free NH bands. The reason for the intensity differences becomes clearer based on the spectra discussed next.

**300 K** [YGGFL + H] $^+$ . 2C-IRMPD at Room Temperature. The use of IR-UV DR to record IR spectra becomes unfeasible at room temperature since the electronic spectrum becomes congested and broadened by hot bands at the internal energies available to the ion at room temperature. This, in turn, makes it difficult to deplete the UV-induced fragmentation signal via IR absorption. By contrast, the 2C-IRMPD technique relies on the broadening of a given vibrational transition to record nearlinear IR spectra as a fragmentation gain. The vibrational broadening that accompanies IR absorption occurs in a similar fashion for ions initially at 300 K as at 10 K. Figure S1b displays the 1C-IRMPD spectrum at 300 K overlaid with the spectrum of the IR-excited 300 K ions, showing the analogous band broadening that occurs. The scheme used to record the IR-excited spectrum at 300 K is identical with that used to record the 10 K IR-excited spectrum in Figure 1d.

Figures 3e and 3f show 2C-IRMPD spectra of 300 K [YGGFL + H]<sup>+</sup> in the amide I/II and hydride stretch regions, respectively. As the spectra at 300 and 10 K were recorded under identical laser conditions, it is safe to make direct comparisons between them. There are several noteworthy points to be made based on this comparison. First, with both spectra in hand it is possible to gauge the degree of structural

preservation during the collisional cooling from 300 to 10 K. The relative conformational distribution of peptide ions at 10 and 300 K have been investigated previously by our group for [YAPGA + H]<sup>+</sup>, where we concluded that the number of conformations and their distribution are largely preserved upon cryo-cooling. This conclusion is supported upon comparison of the 300 K spectra to the 10 K spectrum, as the spectral patterns are largely preserved in both regions. We conclude on this basis that even at room temperature [YGGFL + H]<sup>+</sup> remains in a single H-bonded structure, the charge-stabilized type II'  $\beta$ -turn.

Having demonstrated this structural preservation, we do note some subtle changes with temperature. For instance, at 300 K the C10 NH stretch transition in the hydride stretch region shifts 20 cm<sup>-1</sup> higher in frequency than its position at 10 K. Concomitantly, at 300 K the Phe C=O stretch in the amide I/II shifts 15 cm<sup>-1</sup> to lower frequency. These shifts are both highlighted by using red dashed lines to connect the transitions in Figures 3d-f and Figures 3c-e. The C10 NH··· O=C H-bond closes the  $\beta$ -hairpin turn (see Figure 1), and the shift to higher frequency at room temperature indicates that this bond is weakened with increasing internal energy, suggesting a slight loosening of the  $\beta$ -hairpin turn. At the same time, the Phe C=O acts as a H bond acceptor from the carboxylic acid OH. The shift of this fundamental to lower frequency is consistent with a modest strengthening of this Hbond. The ability to gauge the nature and magnitude of the structural changes that occur during the cooling process is a substantial advantage of 2C-IRMPD. Furthermore, the method provides additional evidence that mid-sized peptide ions such as [YGGFL + H]+ will often retain their room temperature structures and populations during the collisional cooling process.4

Effect of IRMPD Transparency on 1C-IRMPD Spectra. We noted previously that the C10 NH band was absent in the 1C-IRMPD spectrum at 300 K. In the previous section it was noted that this band was sensitive to the ion's internal energy content, displaying a 20 cm<sup>-1</sup> shift from its position at 10 K when warmed to 300 K. This 20 cm<sup>-1</sup> shift explains its absence in the 1C spectrum when starting at 10 K. A single photon at 3310 cm<sup>-1</sup> (peak absorption at 10 K) gives the ion approximately half the average internal energy it possesses at 300 K, most likely shifting the band out of resonance after absorption of a single photon.

The absence of the C10 NH stretch fundamental in [YGGFL + H]<sup>+</sup> demonstrates that "IR transparency" can affect even ions that have a single dominant conformation over the range from 10 to 300 K. Furthermore, its absence at 300 K indicates that the C10 fundamental continues to shift in frequency after IR absorption when starting at 300 K. We see this as evidence that care should be taken when using IRMPD to record spectra of conformationally flexible ions, as missing transitions could prevent correct structural assignments.

It was not feasible to record 1C-IRMPD spectra at either temperature in the amide I/II region due to insufficient IR laser power in that wavelength region ( $\sim 300~\mu J/\text{pulse}$ ). This is a disadvantage of the table-top IR lasers used in our 2C-IRMPD scheme. It is worth noting, however, that the Phe C= O band that was shown to be sensitive to the ion's internal energy content is also only weakly present in the IRMPD spectra of [YGGFL + H]<sup>+</sup> taken with a free electron laser. Recall that this band shifted 15 cm<sup>-1</sup> lower in frequency upon warming the ion to 300 K.

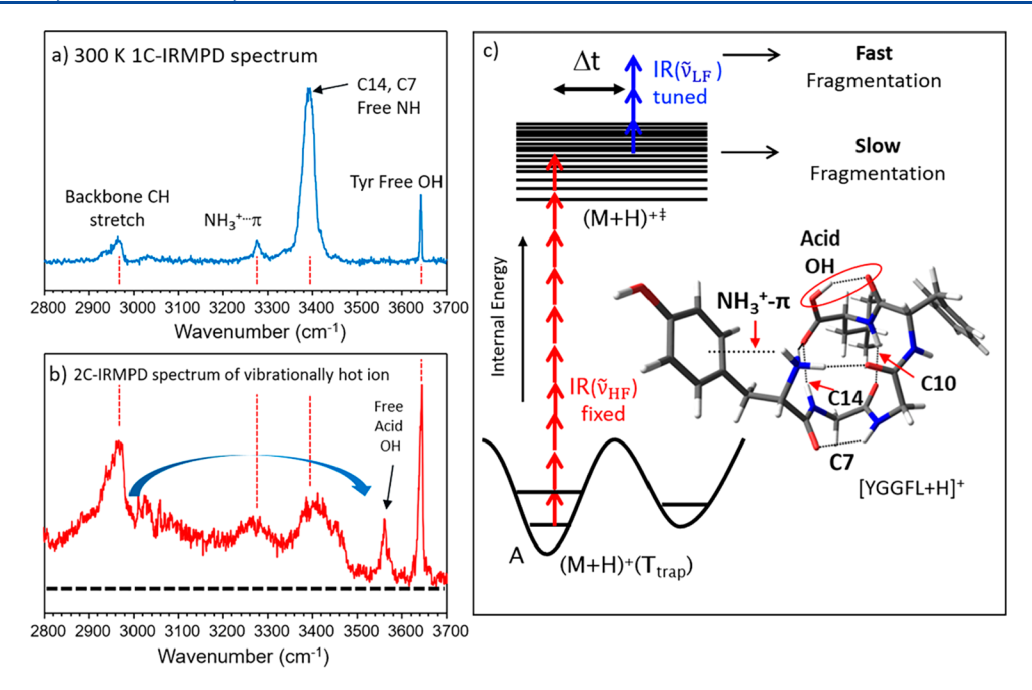


Figure 4. (a) 1C-IRMPD spectrum of YGGFL taken at 300 K. (b) 2C-heated IRMPD spectrum of YGGFL taken from 300 K ions. (c) 2C-heated IRMPD laser scheme with the assigned starting structure for [YGGFL + H]<sup>+</sup> as an inset.

[YGGFL + H]<sup>+</sup> at High Internal Energies. In the previous section it was asserted that the C10 stretch is absent in the 1C spectrum at room temperature because its absorption frequency shifts as the internal energy is raised. By slightly modifying the 2C-IRMPD scheme, it is possible to record the IR spectrum of ions that have been heated to internal energies far greater than what is available to them at room temperature. The comparison of the spectrum at high internal energies to that at 300 K can be used to reveal the isomerization and associated frequency shifts that take place as ions approach and exceed the fragmentation threshold.

The new scheme is depicted in Figure 4c, which we refer to as 2C-heated IRMPD. This scheme is in contrast to the 2C-IRMPD scheme shown in Figure 1d and to the photoexcited scheme previously described<sup>36</sup> as many IR photons (up to  $\sim$ 13, as we will show) are absorbed by the ion prior to recording the vibrational spectrum. In this scheme the highfluence laser is fixed on a resonant transition present in the 1C spectrum and timed to irradiate the ion packet first, followed by the low-fluence laser which is tuned. The spectrum shown in Figure 4b was recorded by using the scheme  $[\lambda_{HF}(3400$ cm<sup>-1</sup>)|30 ns| $\lambda_{LF}$ (tuned)], with  $\lambda_{HF}$  fixed on the most intense band present in the 1C spectrum of Figure 4a. Because the goal of this experiment is to probe the IR spectra of ions at internal energies at or above the dissociation threshold, we chose to start the excitation process from 300 K ions. By fixing  $\lambda_{HF}$  on a transition present in the 1C spectrum, some degree of photofragmentation is induced. The baseline for the signal induced by  $\lambda_{HF}$  is indicated with the black dashed line in Figure 4b. The signal above this dotted line is due to fragmentation induced by  $\lambda_{LF}$ . Oomens et al. have modeled the dynamics of IRMPD to understand the intensity changes present relative to linear spectra and suggest that a Poisson distribution of internal energies is likely present following IVRdominated multiple photon excitation.9 As a result, after irradiation with  $\lambda_{HF}$  some ions in the ion packet have absorbed enough photons to undergo fragmentation on the experimental

time scale whereas the remaining fraction are heated to a lesser degree and fragment either on a slower time scale or not at all. Following a fixed time delay, the low-fluence laser is tuned through the  $2800-3700~\rm cm^{-1}$  region, adding internal energy to the ion through absorption of additional photon(s), as illustrated in Figure 4c.

The number of fragment ions produced when  $\lambda_{LF}$  is on resonance with the Tyr Free OH is about 4 times the fragment signal produced by  $\lambda_{HF}$  (3400 cm<sup>-1</sup>) alone. The photofragments induced by  $\lambda_{LF}$  are a result of  $\lambda_{LF}$  coming into resonance with a vibrational transition present in the conformation or collection of conformations that have been produced by  $\lambda_{HF}$  which have not yet fragmented. In this sense, a 2C-heated IRMPD spectrum probes the changes to the network of H-bonds in the hot ion produced by the  $\lambda_{HF}$ . The corresponding spectrum in the amide I/II region was not recorded because of the lower power available in that region.

To gauge the range of internal energies possessed by the ions that are probed with the 2C-heated IRMPD scheme, Figure 5 shows RRKM rates k(E) for fragmentation (formation of the b<sub>4</sub><sup>+</sup> ion) of [YGGFL + H]<sup>+</sup>, taken from Laskin.<sup>43</sup> In Figure 5, the blue dashed line indicates the average internal energy possessed by the [YGGFL + H]<sup>+</sup> ion at 300 K. The red dashed line indicates the internal energy at which ion fragmentation occurs on the millisecond time scale. The rate of fragmentation reaches  $10^3$  s<sup>-1</sup> at internal energies of about  $\sim$ 5.4 eV or, equivalently,  $\sim$ 13 photons at 3400 cm<sup>-1</sup>. As previously discussed, [YGGFL + H]<sup>+</sup> is estimated to absorb up to two photons from the low-fluence laser when resonant with the IR laser under the conditions used to record the spectrum in Figure 3d. The spectrum in Figure 4b was recorded under similar fluence. The red shaded region in Figure 5 corresponds to the energy range of 6800 cm<sup>-1</sup> (two photons at 3400 cm<sup>-1</sup>) below the energy at which fragmentation occurs on a millisecond time scale. This region corresponds to the range of internal energies the ions must possess to contribute to the additional fragmentation signal induced by  $\lambda_{LF}$ . It is important

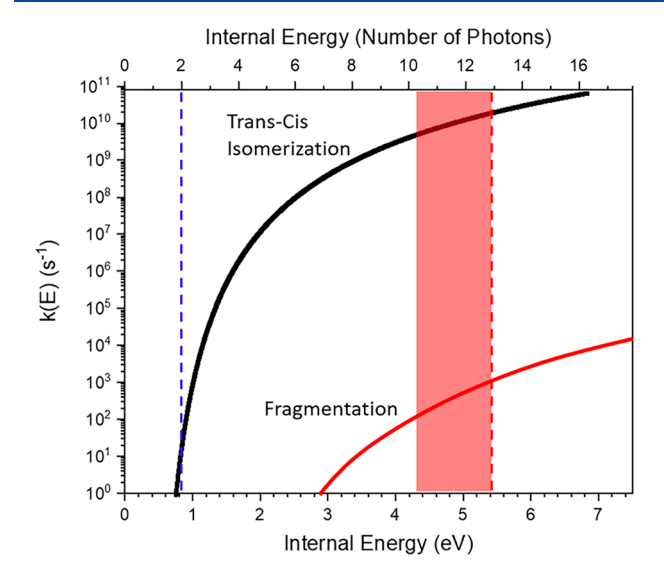


Figure 5. RRKM rate of YGGFL carboxylic acid OH torsion from trans to cis (black curve). Blue and red dashed lines indicate the starting internal energy of the YGGFL ion and the energy at which fragmentation rates (formation of  $b_4^+$  ion) are on a millisecond time scale, respectively. The red highlighted area indicates the estimated range of internal energies possessed by the ions probed by  $\lambda_{\rm LF}$  in the 2C-heated IRMPD scheme. The top x-axis scale corresponds to internal energy in terms of number of photons at 3400 cm<sup>-1</sup>.

to note that the time delay (30 ns) between the lasers will also play a role in limiting what structures are observed. In summary, the spectrum of Figure 4b probes ions that have 4.2–5.4 eV of internal energy, far exceeding the fragmentation thresholds that contribute to thermal dissociation (1–1.5 eV).<sup>43</sup>

The spectrum of the vibrationally hot ions in Figure 4b contains an interesting mixture of absorption types. First, there is evidence that the same transitions that change little in frequency with internal energy at lower energies remain active and relatively sharp in the hot ion spectrum. This is the counterpoint to the statement that vibrational bands that do change their frequency significantly (e.g., those associated with H-bonds that weaken or break) will be "transparent" in 1C-IRMPD spectra.<sup>23</sup> This point is aptly illustrated through comparison of the 300 K 1C-IRMPD spectrum in Figure 4a with the spectrum of the vibrationally hot ions in Figure 4b. Each band that appears in the 1C spectrum has a clear counterpart in the vibrationally hot ion spectrum. The vertical red dashed lines between Figures 4a and 4b connect several transitions in the 1C-IRMPD spectrum (NH<sub>3</sub>+···π, C14, C7, free NH, Tyr OH, and alkyl CH stretch fundamentals) to peaks that appear in broadened form in the vibrationally hot 2C-IRMPD spectrum. Note that since the wavelength of the high-fluence IR source is fixed, the ions that are interrogated with  $\lambda_{LF}$  start from a common distribution of internal energies. Because the ions are quite hot, any distortion of the spectrum due to further changes in the spectral shape with internal energy is likely to be quite small. Thus, the resemblance of the bands in the hot ion spectrum to the initial 10 or 300 K spectra suggests that the dominant conformer population in the hot ion after 30 ns retains certain aspects of its starting structure.

Second, other IR transitions are not obviously present in the hot-ion spectrum. For instance, the C10 NH stretch band that appears at 3330 cm<sup>-1</sup> in the near linear 2C-IRMPD spectrum (Figure 3f) has no identifiable counterpart in the spectrum of

the vibrationally hot ions (Figure 4b), confirming that this band does indeed continue to shift in frequency, broaden, or disappear as the internal energy of the ion is raised.

Third, there is a broad absorption that stretches continuously from 2800 to 3480 cm<sup>-1</sup>. The high-frequency edge at 3480 cm<sup>-1</sup> has a rather sharp cutoff that reflects the fact that free amide NH stretch transitions appear in the 3450-3480 cm<sup>-1</sup> region, with no means of shifting to higher wavenumber. The fact that the absorption intensity in this free amide NH region is small indicates that the vibrationally hot ions that we interrogate have not completely unfolded. Indeed, the absorptions that stretch down to 2800 cm<sup>-1</sup> indicate that some of the strongest H-bonds are still intact, at least to some degree. In the 10 K 2C spectrum (Figure 3d), the absorptions below 3200 cm<sup>-1</sup> have contributions from the H-bonded COOH, the two NH3+····O=C H-bonds, and the alkyl CH stretches. As discussed further below, it seems likely that, apart from the alkyl CH stretch transitions around 2950 cm<sup>-1</sup>, the broad absorption that fills in the 2800-3200 cm<sup>-1</sup> region is largely due to the  $NH_3^+$  group, which sits atop the  $\beta$ -turn and binds to the C-terminal C=O group and the Gly(3) C=O at the center of the turn. The distribution of structures probed by the low-fluence IR laser has loosened, but not broken, these strong ion-carbonyl interactions.

Finally, the most striking feature in the hot-ion spectrum in Figure 4b is the new band that appears at 3560 cm<sup>-1</sup> which has no counterpart in the 1C spectrum. Based on its frequency, this new band is assigned to the fundamental of a free carboxylic acid OH stretch.<sup>19</sup> The presence of this free OH stretch transition is especially interesting, as the starting structure shown in the inset of Figure 4c is one in which the COOH group is trans, with the OH engaged in a strong C7 Hbond with the neighboring C=O group. In the assigned structure the bound OH stretch transition in the cold ion spectrum (Figure 3b) appears as a broad absorption near 2900 cm<sup>-1</sup>. Superimposed on the broad absorption assigned to the OH stretch are much sharper absorptions that are assigned to alkyl CH stretches.2 The appearance of the free acid OH fundamental at 3560 cm<sup>-1</sup> in the hot ion spectrum suggests that the absorption near 2900 cm<sup>-1</sup> in the 1C spectrum and that in the spectrum of the vibrationally hot ions in Figures 4a and 4b, respectively, are a combination of the NH<sub>3</sub><sup>+</sup> hydrogen bonds and alkyl CH's. While alkyl CH stretches do not have particularly strong oscillator strengths, their frequencies are not expected to shift significantly as the ion is heated and isomerization occurs. This provides an ideal scenario for multiphoton absorption.

The blue arrow in Figure 4b denotes the  $\sim$ 660 cm<sup>-1</sup> shift in the frequency of the carboxylic acid OH stretch fundamental from the bound to free position. We have stated previously that the structure of the hot ion retains certain aspects of its starting structure at these elevated internal energies. However, it is simply not possible to assign the spectrum to a single conformation, nor would we anticipate that this would be so. Indeed, it is clear that the acid OH does move to a free position. To estimate the energy barrier needed to break the trans COOH···O=C H-bond, we calculated a relaxed potential energy curve along the OH torsional coordinate that moves the COOH from the trans to the cis position. The calculated transition state for breaking this H-bond to form cis COOH is about 0.53 eV (4240 cm<sup>-1</sup>) above the ground state (see Figure S2 for details). For reference, the lowest energy threshold for fragmentation is 1.14 eV.<sup>43</sup> The rate of the OH group breaking its H-bond during its torsion from the *cis* to the *trans* position is given as a function of internal energy by the black curve in Figure 5. At 3 eV the OH isomerization rate predicted by RRKM calculations (see the Supporting Information) is already on the order of 10<sup>8</sup> s<sup>-1</sup>, consistent with this process occurring during the 30 ns delay between pump and probe lasers.

Taken together, the lower energy threshold for isomerization and the experimental observation of the free acid OH stretch demonstrate that single-step isomerization rates are considerably faster than the ion fragmentation rate. For reference, based on the equilibrium constants at 300 K (0.83 eV) and 4.3 eV, it can be estimated that the structure with the unbound COOH accounts for only 5% of the total population at room temperature and 75% or greater of the total population in the energy range probed by  $\lambda_{LF}$  in Figure 4b. Simple rearrangements such as trans-cis COOH isomerization change the nature and strength of the intramolecular H-bonds in the Hbonded network. Given the large frequency shift of the OH stretch between cis and trans positions, this isomerization breaks what is almost certainly the strongest H-bond between neutral groups in the folded ion. At the same time, the presence of strongly shifted absorptions due to the NH<sub>3</sub><sup>+</sup> group indicates that it is bound in such a deep pocket that even with 5 eV internal energy, it retains significant H-bonds with nearby C=O groups on the nanosecond time scale. Therefore, the hot ion spectrum in Figure 4b is of a partially unfolded [YGGFL + H]<sup>+</sup> ion following IR excitation to energies 4 times the threshold for breaking chemical bonds in the ion.

2C-IRMPD on [YGPAA + H]+: A Multiconformer **System.** One of the expectations for spectroscopic studies of large biomolecular ions in the gas phase is that many of these ions will exist in more than one conformation. In this sense [YGGFL + H]+ is more the exception than the rule. Thus, conformer specificity is a highly attractive feature for any spectroscopic technique, including 2C-IRMPD. This is routine in IR-UV DR as the UV spectra of the different conformations are generally resolved and thus have transitions that can serve as monitor transitions for specific conformations. 19 2C-IRMPD requires the presence of IR transitions unique to each conformation, much as in messenger tagging.  $^{44}\ \hat{\ln}$  this section we report a method that achieves conformer specificity by selectively detecting the intermediate state formed by IR excitation on the nanosecond time scale for the delay between the two IR laser pulses.

To demonstrate both the success and challenges of obtaining conformer-specific spectra, we use the singly protonated YGPAA pentapeptide, [YGPAA + H]<sup>+</sup>, as an example. This ion has been shown by previous IR-UV DR studies to adopt two major conformations. <sup>19</sup> These two conformational families, with structures shown in Figure S3, differ primarily in the *cis* vs *trans* geometry of the carboxylic acid OH. These changes in structure also modulate the strengths of the hydrogen bonds involving this group, leading to conformation-specific shifts in the IR spectrum. <sup>19</sup> The conformer-specific IR-UV DR spectra for conformer B (*cis*) and A (*trans*) are reproduced in Figures 6a and 6b, respectively.

It is possible to record a nonconformer-specific spectrum that resembles the composite of the two spectra shown in Figure 6a,b. This is done by choice of an IR transition shared by the two conformers as the fixed wavelength for the high-fluence IR laser used in the fragmentation step.

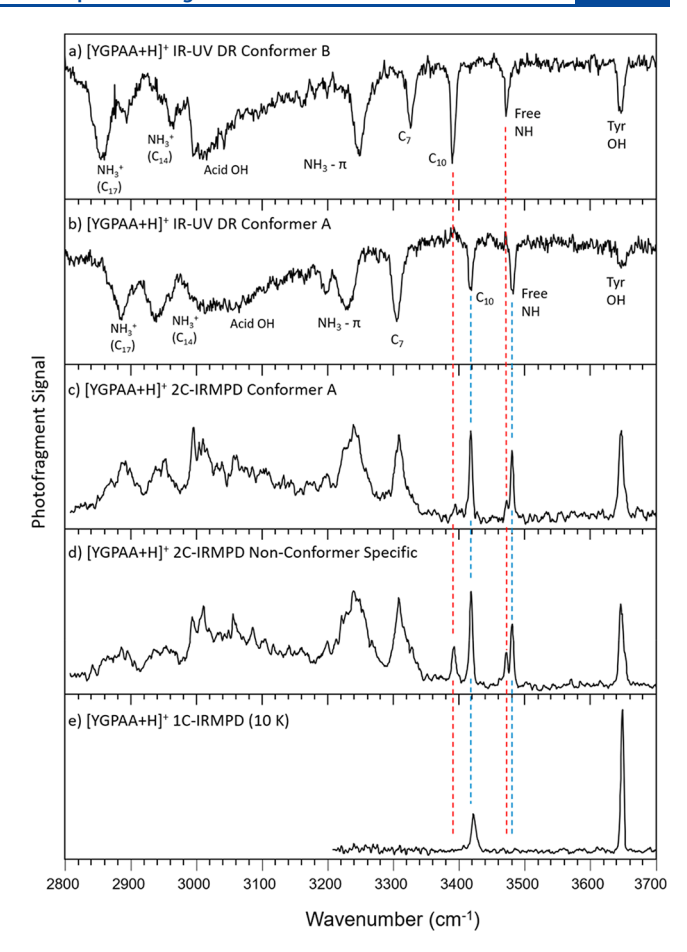


**Figure 6.** Conformer-specific IR-UV DR of [YGPAA + H]<sup>+</sup> conformer B and A, (A) and (B), respectively. Conformer-specific 2C-IRMPD of [YGPAA + H]<sup>+</sup> conformer A (C). Non-conformer-specific 2C-IRMPD of [YGPAA + H]<sup>+</sup> (D). 1C-IRMPD spectrum of [YGPAA + H]<sup>+</sup> taken at 10 K.

For reference, the 1C-IRMPD spectrum taken at 10 K is displayed in Figure 6e between 3200 and 3700 cm<sup>-1</sup>. Interestingly, in this region only two hydride stretch fundamentals appear: the C10 NH stretch of conformer A at 3421 cm<sup>-1</sup> and the free Tyr OH possessed by both conformations at 3650 cm<sup>-1</sup>. To record the composite spectrum shown in Figure 6d, we use the 2C-IRMPD laser scheme [ $\lambda_{LF}$ (tuned)|30 nsl $\lambda_{HF}$ (3645 cm<sup>-1</sup>)]. In this case the high-fluence laser was fixed at a slightly lower wavenumber than the frequency of the shared tyrosine OH stretch, as this band was revealed to broaden toward lower frequency in the spectrum of the IR-excited ions. Fixing  $\lambda_{HF}$  just off resonance from a shared band produces fragmentation from both conformations which we monitor simultaneously. Red and blue connecting lines are drawn from the conformer-specific spectra of conformers B and A, respectively, to the 2C-IRMPD composite spectrum in the region where the differences between spectra are most obvious.

To record a conformer-specific IR spectrum with the 2C-IRMPD technique, it is necessary to selectively monitor the fragmentation of a single conformation by using  $\lambda_{\rm HF}$ . The presence of the C10 band of conformer A in the 1C-IRMPD spectrum provides a means for selective excitation of Conformer A following its selective excitation with  $\lambda_{\rm LF}$ . From the IR excited 2C spectrum it was found that this C10 band broadens on its high-frequency edge as conformer A is heated.

By use of the 2C scheme [ $\lambda_{LF}$ (tuned)|5 nsl $\lambda_{HF}$ (3426 cm<sup>-1</sup>)], it is possible to generate the conformer-specific spectrum of conformer A displayed in Figure 6c. One important aspect of recording this conformer-specific spectrum is that the time delay between the lasers was shortened to 5 ns, the shortest delay possible without temporally overlapping the laser pulses.

To our knowledge, this is the first single-conformer IR spectrum obtained exclusively via an IRMPD approach without any preselection step, such as ion mobility. The short time delay between the two laser pulses was chosen so that isomerization from B into A does not contribute significantly to the spectrum of the IR-excited ion. The blue connecting lines from the conformer specific IR-UV DR spectrum of conformer A (Figure 6b) shows that the transitions that appear in the conformer-specific 2C-IRMPD spectrum in Figure 6c are indeed from conformer A. The red connecting lines show that there is a negligible contribution to the spectrum from conformer B with a 5 ns delay. When this delay was increased to 30 ns, there was a measurable contribution from conformer B (Figure SSc), indicating that A  $\rightarrow$  B isomerization occurs on that time scale at the  $\lambda_{LF}$  laser fluence used.

In our studies of [YGGFL + H]<sup>+</sup>, we surmised that only the bands that do not shift in frequency as a function of internal energy will appear in the 1C-IRMPD spectrum. In the two-conformer case of [YGPAA + H]<sup>+</sup> we see that only two bands appear in the frequency range 3200–3700 cm<sup>-1</sup> starting from 10 K ions at the laser fluences used. The lack of bands unique to conformer B ultimately limits the ability to record a conformer-specific spectrum of conformer B with the 2C-IRMPD technique. Figure S4e and S4f show the 1C-IRMPD spectrum and 2C near-linear IRMPD spectrum of [YGPAA + H]<sup>+</sup> starting from 300 K ions, respectively. These spectra compared to the conformer specific spectra of conformer B show that frequency shifts as a function of internal energy ultimately prevent bands specific to conformer B from appearing in the 1C spectrum at 10 and 300 K.

It is noteworthy that based on the 1C-IRMPD scan alone with its missing transitions, it would not be possible to recognize the presence of two conformers in this sample. The intriguing differences between conformers A and B that enable conformer-specific infrared spectra of A but not B motivate future studies aimed at understanding the conformer-specific dynamics that precedes fragmentation.

## **IV. CONCLUSIONS**

The present work has established the versatile capabilities of the dual OPO variant of 2C-IRMPD as a technique for studying the infrared spectroscopy of large, conformationally complex ions. We have demonstrated that linear-IR spectra can be obtained at cryogenic temperatures, with all its accompanying benefits of sharp spectra that can be used to make 3D structural assignments. Under favorable conditions, it is possible to record conformer-specific IR spectra. Because the spectra can be generated entirely with IR light, ions of both polarities that do not possess a UV chromophore (Figure S5) can be studied without the need for a tag. Furthermore, the ability to record undistorted IR spectra at variable trap temperatures enables structural changes as a function of temperature to be probed.

Finally, an intriguing aspect of the 2C-IRMPD method is its potential for dynamical studies in which the fluence of the two IR sources and the pump—probe time delay can be varied. In the present work, we have shown the extreme example of a

spectrum of  $[YGGFL + H]^+$  following IR excitation with the high-fluence laser, where the ion internal energy is several times the threshold energy for fragmentation. This spectrum shows evidence for substantial unfolding on the 30 ns time scale, pointing the way for future studies in which a range of peptide ion sizes, internal energies, and time delays are explored to obtain snapshots of the ion as it unfolds in response to increases in internal energy. The ability to tune both IR lasers also provides the potential to perform these experiments in a conformer-selective manner.

## ASSOCIATED CONTENT

## Supporting Information

The Supporting Information is available free of charge at https://pubs.acs.org/doi/10.1021/acs.jpca.1c08388.

Comparison of 1C-IRMPD on nonexcited and IR-excited [YGGFL + H] $^+$  at 10 and 300 K; relaxed potential energy surface scan and energies associated with calculations of k(E) for the trans-cis COOH isomerization in [YGGFL + H] $^+$ ; 2C-IRMPD spectra of anions; known structures for conformers A, B of [YGPAA + H] $^+$ ; data exploring the lack of conformer specific 2C-IRMPD spectra of conformer B of [YGPAA + H] $^+$ ; near-linear 2C-IRMPD spectra of deprotonated [YGGFL-H] $^-$  and [GAIDDL-H] $^-$  (PDF)

## AUTHOR INFORMATION

## **Corresponding Authors**

Timothy S. Zwier — Department of Chemistry, Purdue University, West Lafayette, Indiana 47907-2084, United States; Combustion Research Facility, Sandia National Laboratories, Livermore, California 94550, United States; orcid.org/0000-0002-4468-5748; Email: tszwier@sandia.gov

Scott A. McLuckey — Department of Chemistry, Purdue University, West Lafayette, Indiana 47907-2084, United States; orcid.org/0000-0002-1648-5570; Email: mcluckey@purdue.edu

## **Authors**

Christopher P. Harrilal – Department of Chemistry, Purdue University, West Lafayette, Indiana 47907-2084, United States

Andrew F. DeBlase – Department of Chemistry, Purdue University, West Lafayette, Indiana 47907-2084, United States; orcid.org/0000-0002-5274-9078

Complete contact information is available at: https://pubs.acs.org/10.1021/acs.jpca.1c08388

#### Notes

The authors declare no competing financial interest.

## ACKNOWLEDGMENTS

The authors gratefully acknowledge support for this work from the National Science Foundation Chemical Structure, Dynamics and Mechanisms A program under Grant NSF-CHE 1764148. T.S.Z. acknowledges support from the U.S. DOE, Basic Energy Sciences during manuscript preparation at Sandia. Sandia National Laboratories is a multimission laboratory managed and operated by National Technology and Engineering Solutions of Sandia, LLC., a wholly owned subsidiary of Honeywell International, Inc., for the U.S. DOE

National Nuclear Security Administration under Contract DE-NA0003525.

### REFERENCES

- (1) Nagornova, N. S.; Rizzo, T. R.; Boyarkin, O. V. Highly resolved spectra of gas-phase gramicidin S: a benchmark for peptide structure calculations. *J. Am. Chem. Soc.* **2010**, *132* (12), 4040–4041.
- (2) Burke, N. L.; Redwine, J. G.; Dean, J. C.; McLuckey, S. A.; Zwier, T. S. UV and IR spectroscopy of cold protonated leucine enkephalin. *Int. J. Mass Spectrom.* **2015**, *378*, 196–205.
- (3) Leavitt, C. M.; Wolk, A. B.; Fournier, J. A.; Kamrath, M. Z.; Garand, E.; Van Stipdonk, M. J.; Johnson, M. A. Isomer-Specific IR-IR Double Resonance Spectroscopy of D2-Tagged Protonated Dipeptides Prepared in a Cryogenic Ion Trap. J. Phys. Chem. Lett. 2012, 3 (9), 1099–105.
- (4) Asmis, K. R.; Pivonka, N. L.; Santambrogio, G.; Brümmer, M.; Kaposta, C.; Neumark, D. M.; Wöste, L. Gas-Phase Infrared Spectrum of the Protonated Water Dimer. *Science* **2003**, 299 (5611), 1375–1377.
- (5) Fischer, J. L.; Elvir, B. R.; DeLucia, S. A.; Blodgett, K. N.; Zeller, M.; Kubasik, M. A.; Zwier, T. S. Single-Conformation Spectroscopy of Capped Aminoisobutyric Acid Dipeptides: The Effect of C-Terminal Cap Chromophores on Conformation. *J. Phys. Chem. A* **2019**, 123 (19), 4178–4187.
- (6) Jaeqx, S.; Oomens, J.; Cimas, A.; Gaigeot, M. P.; Rijs, A. M. Gasphase peptide structures unraveled by far-IR spectroscopy: combining IR-UV ion-dip experiments with Born-Oppenheimer molecular dynamics simulations. *Angew. Chem., Int. Ed.* **2014**, 53 (14), 3663–6.
- (7) Woodin, R.; Bomse, D.; Beauchamp, J. L. Multiphoton dissociation of molecules with low power continuous wave infrared laser radiation. *J. Am. Chem. Soc.* **1978**, *100* (10), 3248–3250.
- (8) Polfer, N. C. Infrared multiple photon dissociation spectroscopy of trapped ions. *Chem. Soc. Rev.* **2011**, 40 (5), 2211–21.
- (9) Oomens, J.; Sartakov, B. G.; Meijer, G.; von Helden, G. Gasphase infrared multiple photon dissociation spectroscopy of mass-selected molecular ions. *Int. J. Mass Spectrom.* **2006**, 254 (1–2), 1–19.
- (10) Rijs, A. M.; Oomens, J. Gas-Phase IR Spectroscopy and Structure of Biological Molecules; Springer: 2015; Vol. 364.
- (11) Jasikova, L.; Roithova, J. Infrared Multiphoton Dissociation Spectroscopy with Free-Electron Lasers: On the Road from Small Molecules to Biomolecules. *Chem. Eur. J.* **2018**, *24* (14), 3374–3390.
- (12) Okumura, M.; Yeh, L. I.; Lee, Y. T. Infrared spectroscopy of the cluster ions H+3·(H2)n. *J. Chem. Phys.* **1988**, 88 (1), 79–91.
- (13) Okumura, M.; Yeh, L.; Lee, Y.-T. Vibrational predissociation spectroscopy of hydrogen cluster ions. In *Laser Spectroscopy VII*; Springer: 1985; pp 122–125.
- (14) Lisy, J. M. Infrared studies of ionic clusters: the influence of Yuan T. Lee. J. Chem. Phys. 2006, 125 (13), 132302.
- (15) Khanal, N.; Masellis, C.; Kamrath, M. Z.; Clemmer, D. E.; Rizzo, T. R. Glycosaminoglycan Analysis by Cryogenic Messenger-Tagging IR Spectroscopy Combined with IMS-MS. *Anal. Chem.* **2017**, 89 (14), 7601–7606.
- (16) Boyarkin, O. V. Cold ion spectroscopy for structural identifications of biomolecules. *Int. Rev. Phys. Chem.* **2018**, *37* (3–4), 559–606.
- (17) Rizzo, T. R.; Stearns, J. A.; Boyarkin, O. V. Spectroscopic studies of cold, gas-phase biomolecular ions. *Int. Rev. Phys. Chem.* **2009**, 28 (3), 481–515.
- (18) Page, R. H.; Shen, Y.; Lee, Y.-T. Local modes of benzene and benzene dimer, studied by infrared—ultraviolet double resonance in a supersonic beam. *J. Chem. Phys.* **1988**, *88* (8), 4621–4636.
- (19) DeBlase, A. F.; Harrilal, C. P.; Lawler, J. T.; Burke, N. L.; McLuckey, S. A.; Zwier, T. S. Conformation-Specific Infrared and Ultraviolet Spectroscopy of Cold [YAPAA+H](+) and [YGPAA+H](+) Ions: A Stereochemical "Twist" on the beta-Hairpin Turn. J. Am. Chem. Soc. 2017, 139 (15), 5481–5493.
- (20) Schwarz, H.; Asmis, K. R. Identification of Active Sites and Structural Characterization of Reactive Ionic Intermediates by

- Cryogenic Ion Trap Vibrational Spectroscopy. Chem. Eur. J. 2019, 25 (9), 2112-2126.
- (21) Fischer, K. C.; Sherman, S. L.; Garand, E. Competition between Solvation and Intramolecular Hydrogen-Bonding in Microsolvated Protonated Glycine and  $\beta$ -Alanine. *J. Phys. Chem. A* **2020**, 124 (8), 1593–1602.
- (22) Dietl, N.; Wende, T.; Chen, K.; Jiang, L.; Schlangen, M.; Zhang, X.; Asmis, K. R.; Schwarz, H. Structure and Chemistry of the Heteronuclear Oxo-Cluster [VPO4] •+: A Model System for the Gas-Phase Oxidation of Small Hydrocarbons. *J. Am. Chem. Soc.* **2013**, *135* (9), 3711–3721.
- (23) Yacovitch, T. I.; Heine, N.; Brieger, C.; Wende, T.; Hock, C.; Neumark, D. M.; Asmis, K. R. Vibrational spectroscopy of bisulfate/sulfuric acid/water clusters: structure, stability, and infrared multiple-photon dissociation intensities. *J. Phys. Chem. A* **2013**, *117* (32), 7081–90
- (24) Heine, N.; Yacovitch, T. I.; Schubert, F.; Brieger, C.; Neumark, D. M.; Asmis, K. R. Infrared Photodissociation Spectroscopy of Microhydrated Nitrate—Nitric Acid Clusters NO3—(HNO3)m-(H<sub>2</sub>O)n. *J. Phys. Chem. A* **2014**, *118* (35), 7613—7622.
- (25) Oomens, J.; van Roij, A. J.; Meijer, G.; von Helden, G. Gasphase infrared photodissociation spectroscopy of cationic polyaromatic hydrocarbons. *Astrophys. J.* **2000**, *542* (1), 404.
- (26) Schinle, F.; Jacob, C. R.; Wolk, A. B.; Greisch, J. F.; Vonderach, M.; Weis, P.; Hampe, O.; Johnson, M. A.; Kappes, M. M. Ion mobility spectrometry, infrared dissociation spectroscopy, and ab initio computations toward structural characterization of the deprotonated leucine-enkephalin peptide anion in the gas phase. *J. Phys. Chem. A* **2014**, *118* (37), 8453–63.
- (27) Yeh, L.; Okumura, M.; Myers, J.; Price, J.; Lee, T. Y. Vibrational spectroscopy of the hydrated hydronium cluster ions  $H3O+(H_2O)$  n (n= 1, 2, 3). *J. Chem. Phys.* **1989**, *91* (12), 7319–7330.
- (28) Peiris, D. M.; Cheeseman, M. A.; Ramanathan, R.; Eyler, J. R. Infrared multiple photon dissociation spectra of gaseous ions. *J. Phys. Chem.* **1993**, 97 (30), 7839–7843.
- (29) Watson, C. H.; Zimmerman, J. A.; Bruce, J. E.; Eyler, J. R. Resonance enhanced two-laser infrared multiple photon dissociation of gaseous ions. *J. Phys. Chem.* **1991**, *95*, 6081–6086.
- (30) Altinay, G.; Metz, R. B. Comparison of IRMPD, Ar-tagging and IRLAPS for vibrational spectroscopy of Ag+(CH3OH). *Int. J. Mass Spectrom.* **2010**, 297 (1–3), 41–45.
- (31) Sinha, R. K.; Erlekam, U.; Bythell, B. J.; Paizs, B.; Maitre, P. Diagnosing the protonation site of b2 peptide fragment ions using IRMPD in the X-H (X = O, N, and C) stretching region. *J. Am. Soc. Mass Spectrom.* **2011**, 22 (9), 1645–50.
- (32) Sinha, R. K.; Nicol, E.; Steinmetz, V.; Maitre, P. Gas phase structure of micro-hydrated [Mn(ClO4)]+ and [Mn2(ClO4)3]+ ions probed by infrared spectroscopy. *J. Am. Soc. Mass Spectrom.* **2010**, *21* (5), 758–72.
- (33) Lang, J.; Gaffga, M.; Menges, F.; Niedner-Schatteburg, G. Two-color delay dependent IR probing of torsional isomerization in a [AgL(1)L(2)](+) complex. *Phys. Chem. Chem. Phys.* **2014**, *16* (33), 17417–21.
- (34) Duong, C. H.; Gorlova, O.; Yang, N.; Kelleher, P. J.; Johnson, M. A.; McCoy, A. B.; Yu, Q.; Bowman, J. M. Disentangling the Complex Vibrational Spectrum of the Protonated Water Trimer, H(+)(H<sub>2</sub>O)3, with Two-Color IR-IR Photodissociation of the Bare Ion and Anharmonic VSCF/VCI Theory. *J. Phys. Chem. Lett.* **2017**, 8 (16), 3782–3789.
- (35) Duong, C. H.; Yang, N.; Kelleher, P. J.; Johnson, M. A.; DiRisio, R. J.; McCoy, A. B.; Yu, Q.; Bowman, J. M.; Henderson, B. V.; Jordan, K. D. Tag-Free and Isotopomer-Selective Vibrational Spectroscopy of the Cryogenically Cooled H9O4(+) Cation with Two-Color, IR-IR Double-Resonance Photoexcitation: Isolating the Spectral Signature of a Single OH Group in the Hydronium Ion Core. *J. Phys. Chem. A* **2018**, 122 (48), 9275–9284.
- (36) Yang, N.; Duong, C. H.; Kelleher, P. J.; Johnson, M. A.; McCoy, A. B. Isolation of site-specific anharmonicities of individual water molecules in the  $I \cdot (H \ 2 \ O) \ 2$  complex using tag-free,

- isotopomer selective IR-IR double resonance. Chem. Phys. Lett. 2017, 690, 159–171.
- (37) Redwine, J. G.; Davis, Z. A.; Burke, N. L.; Oglesbee, R. A.; McLuckey, S. A.; Zwier, T. S. A novel ion trap based tandem mass spectrometer for the spectroscopic study of cold gas phase polyatomic ions. *Int. J. Mass Spectrom.* **2013**, 348, 9–14.
- (38) Han, H.; Londry, F. A.; Erickson, D. E.; McLuckey, S. A. Tailored-waveform collisional activation of peptide ion electron transfer survivor ions in cation transmission mode ion/ion reaction experiments. *Analyst* **2009**, *134* (4), 681–689.
- (39) Nosenko, Y.; Menges, F.; Riehn, C.; Niedner-Schatteburg, G. Investigation by two-color IR dissociation spectroscopy of Hoogsteen-type binding in a metalated nucleobase pair mimic. *Phys. Chem. Chem. Phys.* **2013**, *15* (21), 8171–8178.
- (40) Harrilal, C. P.; DeBlase, A. F.; Fischer, J. L.; Lawler, J. T.; McLuckey, S. A.; Zwier, T. S. Infrared Population Transfer Spectroscopy of Cryo-Cooled Ions: Quantitative Tests of the Effects of Collisional Cooling on the Room Temperature Conformer Populations. J. Phys. Chem. A 2018, 122 (8), 2096–2107.
- (41) Burke, N. L.; DeBlase, A. F.; Redwine, J. G.; Hopkins, J. R.; McLuckey, S. A.; Zwier, T. S. Gas-Phase Folding of a Prototypical Protonated Pentapeptide: Spectroscopic Evidence for Formation of a Charge-Stabilized beta-Hairpin. *J. Am. Chem. Soc.* **2016**, *138* (8), 2849–57.
- (42) Polfer, N. C.; Oomens, J.; Suhai, S.; Paizs, B. Infrared spectroscopy and theoretical studies on gas-phase protonated leuenkephalin and its fragments: direct experimental evidence for the mobile proton. *J. Am. Chem. Soc.* **2007**, *129* (18), 5887–5897.
- (43) Laskin, J. Energetics and dynamics of fragmentation of protonated leucine enkephalin from time-and energy-resolved surface-induced dissociation studies. *J. Phys. Chem. A* **2006**, *110* (27), 8554–8562.
- (44) Voss, J. M.; Kregel, S. J.; Fischer, K. C.; Garand, E. IR-IR Conformation Specific Spectroscopy of Na+(Glucose) Adducts. *J. Am. Soc. Mass Spectrom.* **2018**, 29 (1), 42–50.
- (45) Poully, J.-C.; Grégoire, G.; Ballivian, R.; Dugourd, P.; Schermann, J. P. Coupling infrared multiphoton dissociation spectroscopy, mass-spectrometry and ion mobility spectrometry for the determination of structures of angiotensin II cations. *Vib. Spectrosc.* **2011**, *56* (1), 105–109.